Journal of Materials Chemistry A

COMMUNICATION

The general synthesis of Ag nanoparticles anchored on silver vanadium oxides: towards high performance cathodes for lithium-ion batteries†

Cite this: J. Mater. Chem. A, 2014, 2, 11029

Received 24th January 2014
Accepted 9th April 2014

DOI: 10.1039/c4ta00437j

www.rsc.org/MaterialsA

Jiang Zhou,[a] Qiang Liang,[a] Anqiang Pan,*[a] Xuelin Zhang,[a] Qinyu Zhu,[a] Shuquan Liang*[a] and Guozhong Cao*[b]

A general strategy has been developed for the one-pot synthesis of Ag nanoparticles uniformly anchored on silver vanadium oxides (SVOs) including $AgVO_3$, $Ag_2V_4O_{11}$, $Ag_{0.33}V_2O_5$ and $Ag_{1.2}V_3O_8$. All the resulting Ag/SVO hybrids demonstrated excellent lithium ion electrochemical intercalation properties, due largely to the improvement in conductivity with the introduction of silver nanoparticles, the large accessible surface area and possible catalytic effects. For instance, the as-prepared $Ag/AgVO_3$ hybrid exhibits a superior rate capability, with a high discharge capacity of 199 mA h g^{-1} even at a rate of 5 A g^{-1}.

Having the most complicated phases among the metal oxides, silver vanadium oxides (SVOs) with a number of phases can be obtained using variations in reaction conditions and material stoichiometry. SVOs with different ratios of silver, vanadium, and oxygen, may display subtly different physicochemical properties, such as electrochemical properties, sensing properties, catalytic activity, optical properties, magnetic properties, electrical properties, and so on.[1–9] In particular, SVOs with a variety of oxidation states have found a suitable application in lithium batteries. SVOs as cathode materials possess a high capacity and energy density, compared to traditional cathode materials, and thus attract many researchers' attention.[1] SVOs are considered firstly as cathode materials for primary lithium batteries, because of their high energy density and unsatisfactory cycling behavior. For example, $Ag_2V_4O_{11}$ has been commercially used as a cathode material in primary lithium batteries for power implantable biomedical devices. Very recently, many groups[3,10–13] have developed nanostructured $AgVO_3$ to improve the cycling performance and rate capability of $AgVO_3$ materials. Other silver vanadium oxides, such as $Ag_{0.33}V_2O_5$ and $Ag_{1.2}V_3O_8$, have also been explored as cathode materials in rechargeable lithium batteries.[6,14,15] However, their rate capability and cyclic stability are unsatisfactory and still need further improvement.

It is believed that an effective approach to obtaining an enhanced electrochemical performance is synthesizing SVOs anchored with silver nanoparticles, because of the improvement in conductivity caused by the metallic silver.[16] Moreover, the Ag/SVO hybrids also can find applications in sensors, catalysts, antibacterial agents, water-based paints, surface-enhanced Raman spectroscopy, *etc.*[5,13,17–21] However, it is difficult to synthesise Ag nanoparticles anchored on metal oxides with high oxidation states, such as SVOs. Moreover, to the best of our knowledge, there is no general strategy for the preparation of a series of SVOs ($AgVO_3$, $Ag_2V_4O_{11}$, $Ag_{0.33}V_2O_5$ and $Ag_{1.2}V_3O_8$). Therefore, to develop a general method for the synthesis of uniform Ag nanoparticles anchored on a series of SVOs is challenging, and would be of great interest to the scientific community.

In this work, we have developed a facile, general and scalable strategy to prepare Ag nanoparticles anchored on silver vanadium oxides (SVOs), including $AgVO_3$, $Ag_2V_4O_{11}$, $Ag_{0.33}V_2O_5$ and $Ag_{1.2}V_3O_8$. In brief, NH_4VO_3 powder first reacts with H_2O_2 in deionized water to form a bright-yellow solution, and this is followed by the addition of a stoichiometric amount of $AgNO_3$. The resulting homogeneous solution is dried to get solid precursors, which are further calcined in air at various temperatures to obtain the final products. Various silver vanadium oxides ($AgVO_3$, $Ag_2V_4O_{11}$, $Ag_{1.2}V_3O_8$, $Ag_{0.33}V_2O_5$) can be fabricated by tuning the ratio of V to Ag. A detailed experimental section can be found in the ESI.† The as-synthesized Ag/SVO hybrids exhibit enhanced electrochemical properties. For example, a high specific discharge capacity of 199 mA h g^{-1} can be delivered for the $Ag/AgVO_3$ hybrid even at an ultra-high discharge current density of 5 A g^{-1}. Additionally, a rechargeable $Ag/Ag_{0.33}V_2O_5$ hybrid electrode shows a remarkable capacity retention of 96.4% after 200 cycles at 300 mA g^{-1}.

The $AgVO_3$ oxides have three typical crystallographic forms: α-$AgVO_3$, β-$AgVO_3$ and γ-$AgVO_3$.[22] However, α-$AgVO_3$ is metastable

[a]School of Materials Science and Engineering, Central South University, Changsha 410083, P. R. China. E-mail: pananqiang@gmail.com; lsq@mail.csu.edu.cn

[b]Department of Materials Science & Engineering, University of Washington, UW, 98195, USA. E-mail: gzcao@u.washington.edu

† Electronic supplementary information (ESI) available. See DOI: 10.1039/c4ta00437j

and will irreversibly transform into the stable β-$AgVO_3$ phase at around 200 °C, and the fabrication of γ-$AgVO_3$ always requires high temperatures.[23] β-$AgVO_3$ is structured as a strong three dimensional network of V_4O_{12} double chains, held together by AgO_6 octahedra and firmly interconnected by Ag_2O_5 and Ag_3O_5 square pyramids.[22,24] Not only the structural stability, but also the peculiar physicochemical properties of the stable phase of β-$AgVO_3$ have attracted increasing attention in recent years. In our work, the Ag-anchored β-$AgVO_3$ in the monoclinic system of the space group of $I2/m$(12) can be synthesized at a wide range of temperatures. TG-DSC results suggest that the Ag/$AgVO_3$ hybrid can be readily synthesized at 350 °C (ESI, Fig. S1†), because no obvious peaks have been detected between 329 °C and 468 °C. This has been confirmed by the XRD patterns shown in Fig. 1a. All diffraction peaks in the XRD patterns can be well indexed as the monoclinic β-$AgVO_3$ phase (JCPDS card no. 29-1154),[2,5,8] and no new phases are generated in the examined temperature range. XPS techniques were further employed to study the β-$AgVO_3$ phase (ESI, Fig. S2†). It is interesting to find that the Ag 3d region can be divided into two peaks, of Ag 3d (5/2) and Ag 3d (3/2), indicating the presence of different valence states for the silver species (Fig. 1b). The two strong peaks at the Ag regions of 367.4 and 373.4 eV can be assigned to Ag^+ Ag 3d (5/2) and Ag 3d (3/2), respectively, while the two relatively weak peaks located at 368.4 and 374.4 eV can be attributed respectively to Ag^0 Ag 3d (5/2) and Ag 3d (3/2).[11] These results demonstrate the co-existence of Ag^0 and $AgVO_3$ (Ag^+) in the obtained materials. Recently, many groups have reported that the metallic silver in the active material can result in a significant increase in conductivity, leading to an enhanced electrochemical performance of the materials as cathode materials for lithium ion batteries.[16,25,26]

The synthesized β-$AgVO_3$ is of a rod-like shape, with a diameter of around 200–500 nm, and many white nanoparticles are anchored on the surface of the material (ESI, Fig. S3†). The detailed structures were investigated using TEM, and the results are shown in Fig. 1c. A large number of nanoparticles are uniformly distributed on the surface of the $AgVO_3$ nanorod. The diameter of an individual nanoparticle is less than 20 nm. The corresponding high-resolution transmission electron microscopy (HRTEM) image (Fig. 1d) confirms that the nanoparticles are Ag nanoparticles, due to the clear lattice spacing of ≈0.236 nm, corresponding well to the lattice spacing of the (111) plane of the cubic Ag phase [JCPDS card no. 04-0783]. In addition, the marked *d*-spacing of ≈0.276 nm and ≈0.305 nm of the lattice fringes correspond to the distances of the (−411) and (310) planes of the monoclinic β-$AgVO_3$ phase. These results correspond well with the previous XPS result, which confirms the existence of an Ag phase. It is safe to believe that the Ag/$AgVO_3$ hybrid has been successfully prepared by our simple synthesis approach.

The Ag/$AgVO_3$ hybrid calcined at 400 °C in air for 4 h is assembled into coin-cells to evaluate its electrochemical properties. Fig. 2a shows the initial cyclic voltammetry (CV) curve for the Ag/$AgVO_3$ hybrid. Three strong cathodic peaks at 2.97, 2.32, and 2.16 V *vs.* Li/Li^+ and one weak cathodic peak at 1.95 V *vs.* Li/Li^+ are clearly observed. All the cathodic peaks are associated with the continuous reduction of Ag^+ to Ag^0; the cathodic peaks at 2.32 and 2.16 V *vs.* Li/Li^+ are attributed to the reduction of V^{5+} to V^{4+} and the partial reduction of V^{4+} to V^{3+}, respectively.[11,12,22,27,28] The weak cathodic peak at 1.95 V *vs.* Li/Li^+ may be ascribed to the further reduction of vanadium from V^{4+} to V^{3+}.[29] Fig. 2b shows the discharge curves of the Ag/$AgVO_3$ hybrid electrodes at different current densities. The electrodes deliver

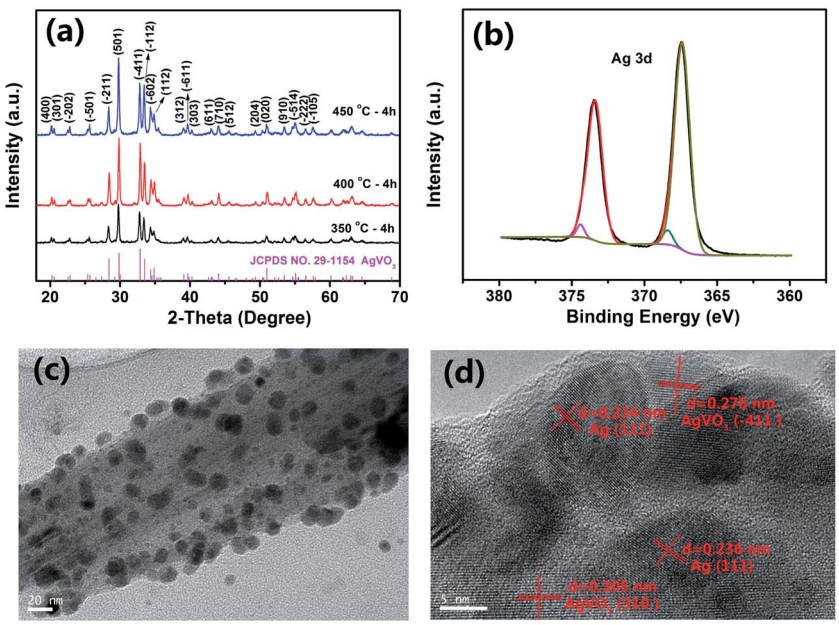

Fig. 1 (a) XRD patterns of Ag/$AgVO_3$ hybrids prepared at different temperatures; (b) X-ray photoelectron spectroscopy results for the Ag 3d states in the Ag/$AgVO_3$ hybrid obtained at 400 °C for 4 h; (c) TEM image and (d) HRTEM image of an individual Ag/$AgVO_3$ nanorod prepared at 400 °C for 4 h.

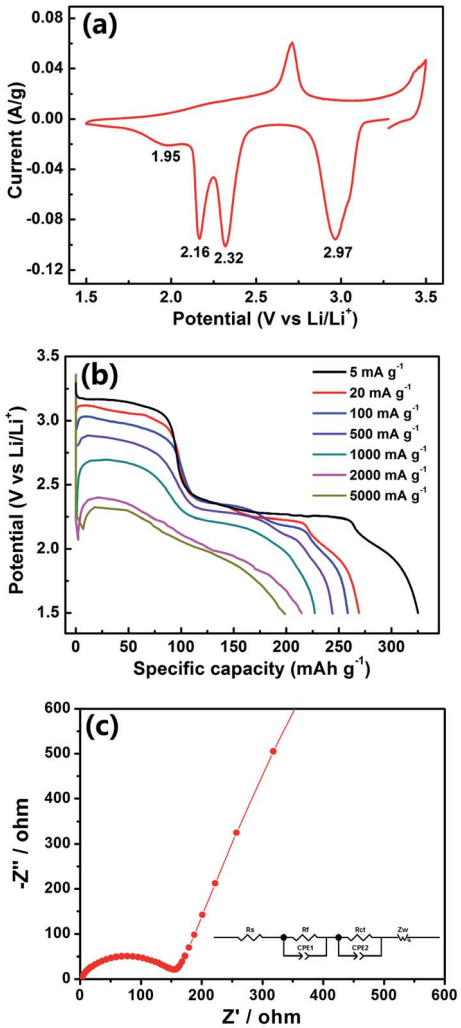

Fig. 2 (a) Initial cyclic voltammetry (CV) curve, (b) initial discharge curves at different current densities and (c) Nyquist plot for the Ag/$AgVO_3$ hybrid prepared at 400 °C for 4 h. The inset of (c) shows the equivalent circuit model for the impedance spectra.

high specific discharge capacities of 325, 269, 259, 244, 227 and 215 mA h g^{-1} at the current densities of 5, 20, 100, 500, 1000 and 2000 mA g^{-1}, respectively. Surprisingly, even at an ultra-high discharge current density of 5000 mA g^{-1}, the hybrid still exhibits a high specific discharge capacity of 199 mA h g^{-1}. It has a capacity retention of 74% when the current density is raised from 20 mA g^{-1} to 5000 mA g^{-1} (ESI, Fig. S4†), indicating a superior rate capability for the silver nanoparticles anchored on the $AgVO_3$ electrode. Electrochemical impedance spectroscopy measurements were also carried out, and the simulation charge-transfer resistance was found to be 117 Ω. This is much smaller than those reported for other $AgVO_3$ electrodes, including $AgVO_3$/PANI triaxial nanowires,[10] Ag/$AgVO_3$ hybrid nanorods[12] and polyaniline-coated β-$AgVO_3$ nanowires.[30] This smaller charge-transfer resistance may be due to the high electronic conductivity of the as-prepared hybrid electrode, resulting in faster electron transportation. The excellent rate capability of the Ag/$AgVO_3$ hybrid can be attributed to the following possible mechanisms: (1) Ag nanoparticles anchored on $AgVO_3$ nanorods, and the Ag generated *in situ* from $AgVO_3$ during the discharge process (ESI, Fig. S5†), result in an enhanced electron conductivity, (2) ample space between the nanostructured materials would facilitate electrolyte penetration, and (3) the Ag nanoparticles may have catalytic effects which improve the intercalation–de-intercalation reaction at the surface. As shown in Table S1,† many synthetic methods have been exploited to improve the electrochemical properties of SVO electrodes, and some do demonstrate desirable properties. When compared with the current SVO electrodes, the rate capability of the as-prepared Ag/$AgVO_3$ hybrid is among the best ever reported (ESI, Table S1†). We also evaluated its long-term cycling performance. After 200 cycles, the capacity quickly decreased to 50 mA h g^{-1}, which can be attributed to the intrinsic irreversibility of the $AgVO_3$ electrodes (ESI, Fig. S6†). This capacity fading is attributed to the irreversible phase transition of crystallites upon cycling (ESI, Fig. S5†). However, the high specific discharge capacity and the excellent rate capability of the Ag/$AgVO_3$ hybrid have proven that it is a promising cathode candidate in primary lithium batteries for implantable cardioverter defibrillators (ICDs).

Inspired by the successful preparation of the Ag/$AgVO_3$ hybrid and its good electrochemical properties, other silver vanadium oxides (Ag/$Ag_2V_4O_{11}$, Ag/$Ag_{0.33}V_2O_5$ and Ag/$Ag_{1.2}V_3O_8$) were also generally prepared, using the same preparation strategy and tuning the molar ratios of Ag to V. According to the XRD results (ESI, Fig. S7–S9†), $Ag_2V_4O_{11}$, $Ag_{0.33}V_2O_5$ and $Ag_{1.2}V_3O_8$ are fabricated at various temperatures. The XPS results also provide evidence of the existence of metallic silver (Ag^0) in the as-prepared Ag/SVO hybrids, including in Ag/$Ag_2V_4O_{11}$, Ag/$Ag_{0.33}V_2O_5$ and Ag/$Ag_{1.2}V_3O_8$.

The Ag nanoparticles anchored on silver vanadium oxides (SVOs) were further characterized by transmission electron microscopy (TEM), and the results are shown in Fig. 3. As clearly displayed in the TEM images, all the SVOs are uniformly decorated with many small nanoparticles. The SVOs and the individually anchored nanoparticles were further characterized by HRTEM. The clear lattice fringes with interplanar spacings of ≈0.237 nm (Fig. 3b), ≈0.2056 nm (Fig. 3d) and ≈0.323 nm (Fig. 3f) correspond well to the distances of the (410) plane of the $Ag_2V_4O_{11}$ phase (JCPDS card no. 49-0166), the (204) plane of the $Ag_{0.33}V_2O_5$ phase (JCPDS card no. 81-1740), and the (110) plane of the $Ag_{1.2}V_3O_8$ phase (JCPDS card no. 88-0686), respectively. The HRTEM images of the anchored nanoparticles display clear lattice fringes. This confirms the existence of silver nanoparticles with diameters ranging from 2 to 10 nm.

$Ag_2V_4O_{11}$ material has been commercially used in primary lithium batteries for ICDs because of its high power and long-term (>10 years) stability.[31,32] In the typical $Ag_2V_4O_{11}$ two-dimensional (2D) layered structure, the Ag^+ ions are located between the layers, and infinite $[V_4O_{12}]_n$ quadruple strings, consisting of two in-equivalent vanadium sites, are linked by corner-shared oxygen atoms to provide continuous V–O layers along the (001) plane.[33] In our work, the Ag nanoparticle-anchored $Ag_2V_4O_{11}$ electrodes exhibit relatively high specific capacities of 309 and 272 mA h g^{-1} at 20 and 50 mA g^{-1},

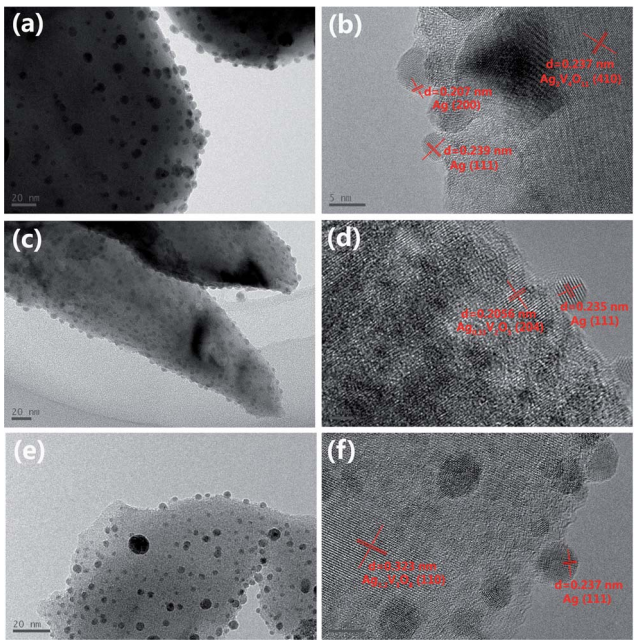

Fig. 3 TEM images and corresponding HRTEM images of the Ag/SVO hybrids: (a and b) $Ag/Ag_2V_4O_{11}$ prepared at 500 °C for 2 h; (c and d) $Ag/Ag_{0.33}V_2O_5$ prepared at 450 °C for 4 h and (e and f) $Ag/Ag_{1.2}V_3O_8$ hybrid prepared at 450 °C for 4 h.

respectively (ESI, Fig. S10†). This electrochemical performance is superior to rheological phase[6] and hydrothermally prepared[7] $Ag_2V_4O_{11}$. However, the capacity of $Ag_2V_4O_{11}$ above 3 V is relatively low when compared to $AgVO_3$ (see Fig. S10† and 2). As ICDs work most efficiently above 3 V, it is important to achieve a higher capacity in this high voltage region, to improve performance for ICDs.[11] In this respect, the $Ag/AgVO_3$ hybrid described in this work, with a superior electrochemical performance, may be more suitable as a cathode for ICDs.

$Ag_{0.33}V_2O_5$, with a monoclinic system and space group of $C2/m(12)$, is composed of V_2O_5 layers and interstitial Ag ions.[34] There are three in-equivalent vanadium sites in the structure of the $Ag_{0.33}V_2O_5$, and the V(3) forms infinite zigzag chains to connect the $[V_4O_{11}]_n$ layers by corner-shared oxygen atoms along the *b*-axis, but in a five-fold square pyramidal coordination ($V(3)O_5$).[33] This unique crystal structure is different from the 2D layered structure of $Ag_2V_4O_{11}$ and results in the 3D tunneled structure of the $Ag_{0.33}V_2O_5$. Compared to $Ag_2V_4O_{11}$ and $AgVO_3$, $Ag_{0.33}V_2O_5$ is much more stable during the lithiation–delithiation process, because the novel 3D tunneled structure can alleviate structural collapse and crystallinity loss. Therefore, among the silver vanadium oxides (SVOs), $Ag_{0.33}V_2O_5$ material has the most potential for use as a cathode material in rechargeable lithium batteries. The electrochemical performance of the $Ag/Ag_{0.33}V_2O_5$ hybrid as a cathode material in rechargeable lithium batteries was evaluated. The initial cyclic voltammetry (CV) curve displays four cathodic peaks and four anodic peaks, indicating the multi-step intercalation–deintercalation of the lithium ions. This is in good agreement with the charge–discharge curves, which have four distinct plateaus observed at about 3.3 V, 3.0 V, 2.5 V and 2.0 V (ESI, Fig. S11†). Fig. 4a shows the cycling performance of the $Ag/Ag_{0.33}V_2O_5$ hybrid at 100 mA g^{-1}. A high initial specific capacity of 220 mA h g^{-1} can be obtained for the $Ag/Ag_{0.33}V_2O_5$ electrode, and 194 mA h g^{-1} is maintained after 50 cycles, with a capacity retention of 88%. The long-term cycling performance (Fig. 4b) indicates that the hybrid exhibits a high specific capacity of 137 mA h g^{-1} at 300 mA g^{-1}, and 132 mA h g^{-1} still can be retained after 200 cycles. This equates to 96.4% of its initial capacity, which is amazing for SVO electrodes. What's more, a high coulombic efficiency of around 99% can be reached. Recent studies have demonstrated good retrievability of the crystal structure of the initial $Ag_{0.33}V_2O_5$, as it can be recovered after several cycles.[6,35] The integrity of the crystal structure of the $Ag_{0.33}V_2O_5$ remains even after 50 cycles (ESI, Fig. S12†). Therefore, the superior electrochemical performance of the $Ag/Ag_{0.33}V_2O_5$ hybrid is attributed to its good structural reversibility and the enhancement in its conductivity with the introduction of Ag nanoparticles.

The typical layered structure of $Ag_{1+x}V_3O_8$ is isostructural with $Li_{1+x}V_3O_8$ in a monoclinic system with the space group of $P2_1/m$.[1] In the $Ag_{1+x}V_3O_8$ layered structure, the $[V_3O_8]_n$

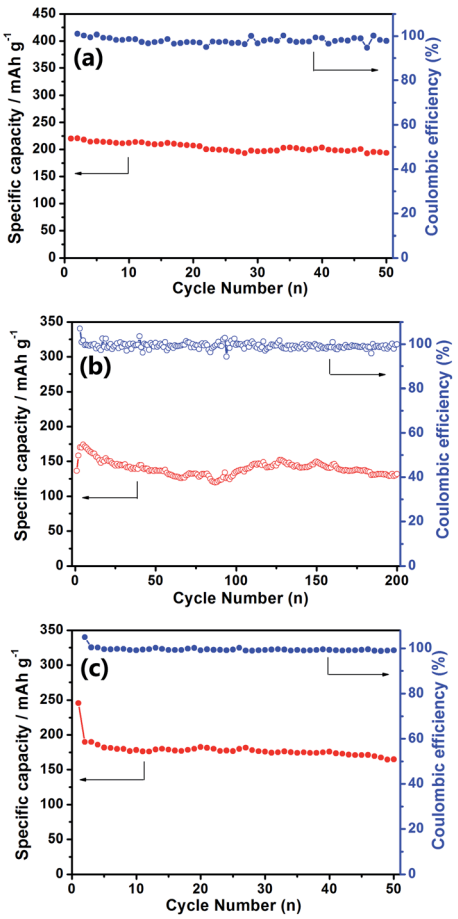

Fig. 4 (a and b) Cycling performance of the $Ag/Ag_{0.33}V_2O_5$ hybrid prepared at 450 °C for 4 h at current densities of 100 mA g^{-1} and 300 mA g^{-1}, respectively. (c) Cycling performance of the $Ag/Ag_{1.2}V_3O_8$ hybrid prepared at 450 °C for 4 h at a current density of 100 mA g^{-1}.

framework is built up around three independent vanadium sites. Two of these are octahedrally coordinated and one has trigonal-bipyramidal coordination, containing two structural units with a double chain of edge-shared trigonal bipyramids connecting the double chains of edge-shared VO_6 octahedra infinitely along the [010] direction. The Ag^+ ions mainly reside in weakly distorted octahedral sites, which is due to the main Li^+ ion sites observed in $Li_{1.2}V_3O_8$.[7,36] During the electrochemical lithiation process, the Ag^+ in the $Ag_{1.2}V_3O_8$ structure will be continuously deposited on the surface of the active material as anchored metallic silver, and the metallic silver is not inserted into the layers during the subsequent lithiation–delithiation process.[15,37] In our recent study, we found that Li^+ ions may replace the Ag^+ ions at the octahedral sites in $Ag_{1.2}V_3O_8$ to form $Li_{1+x}V_3O_8$, and that this structure is reversible upon cycling, which is confirmed by the *ex situ* XRD for the electrodes after the charge–discharge process.[15] The superior cycling performance of $Ag_{1.2}V_3O_8$ over $AgVO_3$ can be attributed to the good structural stability of the $Li_{1+x}V_3O_8$ formed after the first discharge process. The $Ag/Ag_{1.2}V_3O_8$ hybrid is reported for the first time, and its cycling performance as evaluated at 100 mA g^{-1} is displayed in Fig. 4c. A high initial discharge capacity of 246 mA h g^{-1} can be achieved for the electrode, which decreases to 190 mA h g^{-1} in the second cycle. This may due to the successive phase transformations which occur upon lithium ion insertion into the $Ag_{1.2}V_3O_8$, forming the new phase of metallic Ag^0 and $Li_{1+x}V_3O_8$.[15] A stabilized specific discharge capacity of 164 mA h g^{-1} can be obtained after 50 cycles. This good performance is ascribed to the good structural stability of the as-formed $Li_{1+x}V_3O_8$.

Silver vanadium oxides (SVOs), including $AgVO_3$, $Ag_2V_4O_{11}$, $Ag_{0.33}V_2O_5$ and $Ag_{1.2}V_3O_8$, have been obtained by a general strategy in this work. In the past few years, $AgVO_3$ and $Ag_2V_4O_{11}$ materials have been generally investigated as cathodes for primary lithium batteries, while $Ag_{0.33}V_2O_5$ and $Ag_{1.2}V_3O_8$ have been investigated for rechargeable lithium batteries. This is because there are irreversible phase transformations and the formation of an amorphous phase after the first cycle for $AgVO_3$ and $Ag_2V_4O_{11}$, leading to unsatisfactory cycling behavior.[11,12] However, $Ag_{0.33}V_2O_5$ demonstrates excellent structural stability and $Ag_{1.2}V_3O_8$ transfers to the good structural stability phase of $Li_{1+x}V_3O_8$, which makes them potential cathodes for lithium ion batteries.[6,15,37] As is shown in Table S2,†$Ag/AgVO_3$ and $Ag/Ag_2V_4O_{11}$ exhibit high initial discharge capacities and good rate capabilities; especially $Ag/AgVO_3$, for which a high specific discharge capacity of 199 mA h g^{-1} can be achieved even at an ultra-high discharge current density of 5 A g^{-1}, which is desirable for ICDs. Meanwhile, for $Ag/Ag_{0.33}V_2O_5$ and $Ag/Ag_{1.2}V_3O_8$ electrodes, although lower initial discharge capacities are observed at different current densities, good cycling stabilities are displayed, and results are superior to those for $Ag_{0.33}V_2O_5$ nanowires,[6] $Ag_{0.33}V_2O_5$ nanorods,[14] channel-structured $Ag_{0.33}V_2O_5$ nanorods,[38] and belt-like $Ag_{1.2}V_3O_8$.[15]

In summary, a general strategy has been reported for the one-pot synthesis of Ag nanoparticles uniformly anchored on a series of silver vanadium oxides (SVOs), such as $Ag/AgVO_3$, $Ag/Ag_2V_4O_{11}$, $Ag/Ag_{0.33}V_2O_5$ and $Ag/Ag_{1.2}V_3O_8$. The as-obtained Ag/SVO hybrids have demonstrated highly improved electrochemical properties because of the enhanced electron conductivity. For example, the $Ag/AgVO_3$ hybrid exhibits an excellent rate capability: a high specific discharge capacity of 199 mA h g^{-1} can be reached at an ultra-high discharge current density of 5 A g^{-1}. In particular, this method is cost-effective, environmentally benign and scaleable. It is believed that our strategy could probably be applicable for the preparation of other metal vanadium oxides, with great promise for various applications.

Acknowledgements

This work was supported by the National High Technology Research and Development Program of China (863 Program) (Grant no. 2013AA110106), the National Natural Science Foundation of China (Grant no. 51374255), the Lie-Ying Program of Central South University and the Hunan Provincial Innovation Foundation For Postgraduates.

Notes and references

1 K. J. Takeuchi, A. C. Marschilok, S. M. Davis, R. A. Leising and E. S. Takeuchi, *Coord. Chem. Rev.*, 2001, **219–221**, 283–310.
2 J. M. Song, Y. Z. Lin, H. B. Yao, F. J. Fan, X. G. Li and S. H. Yu, *ACS Nano*, 2009, **3**, 653–660.
3 C. Han, Y. Pi, Q. An, L. Mai, J. Xie, X. Xu, L. Xu, Y. Zhao, C. Niu, A. M. Khan and X. He, *Nano Lett.*, 2012, **12**, 4668–4673.
4 F. Sauvage, V. Bodenez, J. M. Tarascon and K. R. Poeppelmeier, *J. Am. Chem. Soc.*, 2010, **132**, 6778–6782.
5 M. R. Parida, C. Vijayan, C. S. Rout, C. S. Suchand Sandeep and R. Philip, *Appl. Phys. Lett.*, 2012, **100**, 121119.
6 W. Hu, X. B. Zhang, Y. L. Cheng, C. Y. Wu, F. Cao and L. M. Wang, *ChemSusChem*, 2011, **4**, 1091–1094.
7 C. Wu, H. Zhu, J. Dai, W. Yan, J. Yang, Y. Tian, S. Wei and Y. Xie, *Adv. Funct. Mater.*, 2010, **20**, 3666–3672.
8 L. Mai, L. Xu, Q. Gao, C. Han, B. Hu and Y. Pi, *Nano Lett.*, 2010, **10**, 2604–2608.
9 R. A. Leising and E. S. Takeuchi, *Chem. Mater.*, 1994, **6**, 489–495.
10 L. Mai, X. Xu, C. Han, Y. Luo, L. Xu, Y. A. Wu and Y. Zhao, *Nano Lett.*, 2011, **11**, 4992–4996.
11 S. Zhang, W. Li, C. Li and J. Chen, *J. Phys. Chem. B*, 2006, **110**, 24855–24863.
12 S. Liang, J. Zhou, A. Pan, X. Zhang, Y. Tang, X. Tan, T. Chen and R. Wu, *J. Power Sources*, 2013, **228**, 178–184.
13 S. Liang, J. Zhou, X. Zhang, Y. Tang, G. Fang, T. Chen and X. Tan, *CrystEngComm*, 2013, **15**, 9869–9873.
14 Y. Wu, P. Zhu, X. Zhao, M. V. Reddy, S. Peng, B. V. R. Chowdari and S. Ramakrishna, *J. Mater. Chem. A*, 2013, **1**, 852–859.
15 S. Liang, T. Chen, A. Pan, J. Zhou, Y. Tang and R. Wu, *J. Power Sources*, 2013, **233**, 304–308.
16 E. S. Takeuchi, A. C. Marschilok, K. Tanzil, E. S. Kozarsky, S. Zhu and K. J. Takeuchi, *Chem. Mater.*, 2009, **21**, 4934–4939.

17 C. Lu, Q. Shen, X. Zhao, J. Zhu, X. Guo and W. Hou, *Sens. Actuators, B*, 2010, **150**, 200–205.
18 R. D. Holtz, A. G. S. Filho, M. Brocchi, D. Martins, N. Duran and O. L. Alves, *Nanotechnology*, 2010, **21**, 185102.
19 M. W. Shao, L. Lu, H. Wang, S. Wang, M. L. Zhang, D. D. Ma and S. T. Lee, *Chem. Commun.*, 2008, 2310–2312.
20 Z. Chen, S. Gao, R. Li, M. Wei, K. Wei and H. Zhou, *Electrochim. Acta*, 2008, **53**, 8134–8137.
21 R. D. Holtz, B. A. Lima, A. G. S. Filho, M. Brocchi and O. L. Alves, *Nanomedicine*, 2012, **8**, 935–940.
22 F. Cheng and J. Chen, *J. Mater. Chem.*, 2011, **21**, 9841.
23 S. Kittaka, K. Matsuno and H. Akashi, *J. Solid State Chem.*, 1999, **142**, 360–367.
24 P. Rozier, J. M. Savariault and J. Galy, *J. Solid State Chem.*, 1996, **122**, 303–308.
25 A. C. Marschilok, E. S. Kozarsky, K. Tanzil, S. Zhu, K. J. Takeuchi and E. S. Takeuchi, *J. Power Sources*, 2010, **195**, 6839–6846.
26 E. S. Takeuchi, A. C. Marschilok, K. J. Takeuchi, A. Ignatov, Z. Zhong and M. Croft, *Energy Environ. Sci.*, 2013, **6**, 1465–1470.
27 Y. K. Anguchamy, J. W. Lee and B. N. Popov, *J. Power Sources*, 2008, **184**, 297–302.
28 J. W. Lee and B. N. Popov, *J. Power Sources*, 2006, **161**, 565–572.
29 L. Liang, H. Liu and W. Yang, *Nanoscale*, 2013, **5**, 1026–1033.
30 S. Zhang, S. Peng, S. Liu, L. Ren, S. Wang and J. Fu, *Mater. Lett.*, 2013, **110**, 168–171.
31 C. L. Schmidt and P. M. Skarstad, *J. Power Sources*, 2001, **97–98**, 742–746.
32 A. M. Crespi, S. K. Somdahl, C. L. Schmidt and P. M. Skarstad, *J. Power Sources*, 2001, **96**, 33–38.
33 Y. Xu, X. Han, L. Zheng, W. Yan and Y. Xie, *J. Mater. Chem.*, 2011, **21**, 14466.
34 Y. Liu, Y. Zhang, M. Zhang and Y. Qian, *J. Cryst. Growth*, 2006, **289**, 197–201.
35 S. Liang, Y. Yu, T. Chen, A. Pan, S. Zhang, J. Zhou, Y. Tang and X. Tan, *Mater. Lett.*, 2013, **109**, 92–95.
36 P. Rozier and J. Galy, *J. Solid State Chem.*, 1997, **134**, 294–301.
37 J. Kawakita, Y. Katayama, T. Miura and T. Kishi, *Solid State Ionics*, 1997, **99**, 71–78.
38 S. Liang, X. Zhang, J. Zhou, J. Wu, G. Fang, Y. Tang and X. Tan, *Mater. Lett.*, 2014, **116**, 389–392.